Published in final edited form as:
Neuropathology. 2014 October ; 34(5): 429–437. doi:10.1111/neup.12121.

Coxsackievirus B4 myocarditis and meningoencephalitis in newborn twins

Stephanie J. Bissel[#1], **Caitlin C. Winkler**[#1], **Joseph DelTondo**[2], **Guoji Wang**[1], **Karl Williams**[2], and **Clayton A. Wiley**[1]

[1]Department of Pathology, University of Pittsburgh School of Medicine, Pittsburgh, Pennsylvania, USA

[2]Allegheny County Medical Examiner, Pittsburgh, Pennsylvania, USA

[#] These authors contributed equally to this work.

Abstract

Coxsackievirus B4 (CB4) is a picornavirus associated with a variety of human diseases, including neonatal meningoencephalitis, myocarditis and type 1 diabetes. We report the pathological findings in twin newborns who died during an acute infection. The twins were born 1 month premature but were well and neurologically intact at birth. After a week they developed acute lethal neonatal sepsis and seizures. Histopathology demonstrated meningoencephalitis and severe myocarditis, as well as pancreatitis, adrenal medullitis and nephritis. Abundant CB4 sequences were identified in nucleic acid extracted from the brain and heart. *In situ* hybridization with probes to CB4 demonstrated infection of neurons, myocardiocytes, endocrine pancreas and adrenal medulla. The distribution of infected cells and immune response is consistent with reported clinical symptomatology where systemic and neurological diseases are the result of CB4 infection of select target cells.

Keywords

congenital infection; coxsackievirus; encephalitis; enterovirus; myocarditis

Correspondence: Clayton A. Wiley, MD, PhD, Department of Pathology, University of Pittsburgh School of Medicine, M8715 South Tower, 200 Lothrop Street, Pittsburgh, PA 15213, USA. wiley1@pitt.edu.

The authors declare there are no conflicts of interest or commercial associations.

SUPPORTING INFORMATION

Additional Supporting Information may be found in the online version of this article at the publisher's web-site:

Figure S1 *CB4 systemic tissue distribution by PCR*. The panenterovirus primer set (see Materials and Methods) was used to amplify CB4 cDNA derived from RNA extracted from brain and systemic tissues from twin A (P1) and twin B (P2). Both twins had robust viral signal in the heart as well as the brain. Note that the viral signal in the brain of P2 is more pronounced than in the brain of P1. Expected product size = 221 base pairs. K = kidney, AG = adrenal gland, S = spleen, P = pancreas, S. Bowel = small bowel, St. = stomach, E = esophagus. Far left column shows molecular weight standards.

Figure S2 In situ hybridization (ISH) for CB4 (A-D) shows multifocal infection throughout the CNS. In addition to infection of cerebral cortex (1F) and germinal matrix regions (2A), infected cells were also observed in the caudate (A), cerebellar deep gray matter (B), midbrain (C) and anterior pituitary (D) All images at 10× magnification, micron bar in 10× = 100 microns.

Table S1 Sources of antibodies used in study.

INTRODUCTION

Of the estimated 20 000 cases of encephalitis that occur annually in the US, more than half are caused by picornaviruses (positive-sense, single stranded RNA (ssRNA), non-enveloped viruses).[1] The genus Enterovirus of the Picornavirus family is divided into 10 species, four of which infect humans. Enteroviruses are remarkable for annual epidemics, some of which, like polio, are notable for neurological disease. With the development of an effective vaccine, polio has been eradicated from much of the globe. However, enteroviruses in general are ubiquitous and account for a majority of viral illnesses worldwide.[2-4] For example, recent Asian epidemics of enterovirus 71 (EV71) have affected millions of individuals.[5] Children younger than 5 years of age are most susceptible to infection, in part due to lack of prior immunity,[6] with infants at risk for more severe clinical disease. From 2006–2008, 1632 enterovirus detections were reported to the National Enterovirus Surveillance System.[7] Of these cases, 47% were reported in children ≤1 year of age. While myocarditis, meningitis and encephalitis are well-recognized complications of enteroviral infection in infants, additional systemic complications have also been observed.

Approximately a quarter of human enteroviral isolates are strains of coxsackievirus.[8] Coxsackie B4 (CB4) is particularly associated with meningoencephalitis in addition to neonatal myocarditis and type 1 diabetes. Since its discovery, there have been scattered reports localizing CB4 in infected organs using a variety of techniques.[9-14] In humans CB4 has displayed a clear tropism for CNS neurons, myocardiocytes and β cells of the pancreas. Infection of human pancreatic β cells *in vitro* is both lytic and nonlytic,[15] and *in vivo* both acute and chronic infections have been described.[16-18] Multiple pathogenic mechanisms of CB4 infection of β cells have been proposed to account for their dysfunction. Less is known regarding infection of myocardiocytes and CNS neurons.

Animal models of coxsackievirus infection have shown some variation in host disease. Early reports of CB4 infection in mice showed the myocardial tropism[19] that was also later shown in non-human primates.[20] Infection of mice is associated with a pancreatitis; however, the exquisite β-cell tropism noted in humans is not replicated in mice where both exocrine and endocrine pancreatitis have been reported.[21,22] The lack of knowledge of CB4 pathogenic mechanisms, including route of infection, cellular tropism and immune response, as well as several links between enterovirus infections and emerging diseases (such as pandemic acute hemorrhagic conjunctivitis, type 1 diabetes, and potential re-emergence of poliomyelitis),[23] presents a clinical need to further our understanding of enteroviruses and their associated tissue and cellular tropism. Here we present our study of twins infected with CB4 who died 2 days apart approximately 1 week after infection. Systemic and neurological diseases appear to be the direct result of CB4 infection and the subsequent immune response.

MATERIALS AND METHODS

Tissues

Systemic tissues were collected at autopsy and samples frozen at −80°C or immersion fixed in phosphate buffered 10% formalin for 2 weeks. Fixed brains were examined grossly before

sectioning in the coronal plane. After cassetting and paraffin embedding, 6 micron-thick sections were cut and stained for routine histological analysis.

Immunohistochemistry

Immunostaining was performed as described elsewhere.[24] Formalin-fixed paraffin-embedded (FFPE) sections containing systemic organs and brain were stained using mouse antiserum against enterovirus. For double-label immunofluorescence, sections were stained using mouse antiserum against enterovirus and rabbit antiserum against specific markers of cell lineage (GFAP, ionized calcium-binding adapter molecule 1 (IBA1), synaptophysin, microtubule-associated protein 2 (MAP2), tyrosine hydroxylase (TH) or CD21). Antibody dilutions are shown in Table S1.

PCR

Nucleic acids were extracted from 100 mg portions of frozen tissue or from scrolls of approximately 10 6 micron-thick sections of paraffin embedded tissues using the QuickExtract FFPE RNA Extraction kit from Epicentre (QFR82050, Madison, WI, USA). cDNA was synthesized from the extracted RNA using the Retroscript kit from Ambion, Grand Island, NY, USA (AM1710). The following primers were designed to amplify 221 base pairs of the 5′ untranslated region (UTR) of the viral genome (a region of high conservation based on a multi-sequence alignment of 30 different species of enterovirus): EVFP, 5′-GCGAAGAGTCTATTGAGC; EVRP, 5′-GATGGCCAATCCAATAGC. Amplified products were sequenced and shown to have 98% homology to CB4 sequence (confirmed by the Centers for Disease Control (CDC) in Atlanta). Additional primers were designed to amplify 291 base pairs of the VP1 region of the CB4 genome: CVFP, 5′-CAAACTCTGAACAAATCCC; CVRP, 5′-TCAACTCCATGTCACACC.

In situ hybridization (ISH)

Riboprobe DNA templates for either the 5′-UTR position 418–638 (GenBank accession no. JX308222) or the capsid protein VP1 position 68–341 (GenBank accession no. JN203601) were used to synthesize both positive and negative sense ^{35}S-labeled riboprobes using Riboprobe Combination System – SP6/T7 RNA Polymerase (Promega, Madison, WI, USA) *in vitro* transcription kit. FFPE tissue sections of brain and systemic organs were deparaffinized with Histoclear and microwaved in 1× Citrate Buffer pH 6.0 (Invitrogen, Carlsbad, CA, USA). Hybridization was carried out as previously described.[25,26] For double-label ISH/immunofluorescence (IF) (MAP-2 or tyrosine hydroxylase), sections were first hybridized as described above and then immunostained using primary and secondary antibody dilutions as shown in Table S1. Because processed CD21-stained follicular dendritic cells are so thin and ISH grains block immunofluorescence, successive paraffin sections of spleen were used for single-label ISH or IF and then aligned and merged for Figure 2D.

RESULTS

Clinical histories

Monochorionic-diamniotic twins were delivered by C-section at 37 weeks gestation to a gravida-4 para-2 22-year-old. Prenatal care was scant; however, antenatal serological testing was negative for herpes simplex virus, human immunodeficiency virus, hepatitis B virus and venereal disease research laboratory test for syphilis (VDRL), but positive for rubella immunoglobulin. Apgar scores were 8 and 9 and both twins did well in the immediate postnatal days. Discharge was delayed until 4 days after delivery because of hypothermia. At home 8 days after delivery, the mother noted severe lethargy in twin A and requested emergency medical support. The twin was found to be unresponsive and apneic, and despite cardiopulmonary resuscitation remained in asystole and was pronounced dead. Twin B was taken to the emergency room 2 days later with severe respiratory distress and hypotension. On admission pupils were fixed and dilated, and despite aggressive resuscitation measures twin B survived less than a day.

Autopsy and histopathological findings

At autopsy, twin A demonstrated patent foramen ovale and ductus arteriosis with 25 cc of bilateral pulmonary effusions. Cultures of lung swabs grew non-speciated enterovirus. The brain weighed 500 g, was grossly normal and showed no lesions or hemorrhages after coronal sectioning. At autopsy, twin B demonstrated no significant gross findings. The brain weighed 450 g and also showed no focal lesions on gross examination.

Routine HE evaluation demonstrated focal subacute pneumonia. Myocardia of both twins showed severe lymphocytic infiltrates (Fig. 1A,B), but the remaining systemic organs showed minimal HE histopathology. Sections of both brains demonstrated immature neuroanatomy consistent with gestational age. There were no hemorrhages or hypoxic ischemic changes. Leptomeninges and perivascular spaces showed moderate lymphocytic infiltrate greater in twin B than twin A. Immunohistochemical analysis demonstrated CD3 T cell infiltration of the heart, brain, pancreas and adrenal medulla (Fig. 1B,E,H,K).

Virus identification

In order to determine the species of the infecting enterovirus, we designed three sets of primers based on a multisequence alignment of 30 enterovirus genomes. Since the 5′-UTR of enteroviruses is highly conserved, we designed general enterovirus primers from this region. After extracting RNA from tissue samples from each twin and synthesizing cDNA, we performed PCR and determined that one primer set (EVFP/EVRP) amplified more robustly than the other sets. We used this primer set (see Methods section) for sequencing. After a BLAST analysis of the sequence results, we were able to identify the enterovirus as CB4. Our identification was independently confirmed by the CDC in Atlanta. Knowing the identity of the virus, we designed new primer sets based on the VP1 capsid protein of CB4. Again, one set (EVFP/EVRP) notably amplified more robustly (see Methods section). Thus, all subsequent studies were conducted using either the general enterovirus primer set or the CB4-specific primer set.

CB4 tissue distribution

Using RT-PCR and ISH we were able to characterize systemic and brain tissue distribution of CB4 in each of the twins (Tables 1,2). For both twins, the heart samples exhibited an abundant amplified product (Fig. S1). Similarly, brain samples from both twins also exhibited abundant amplification, although the signal from twin B was notably stronger than the signal from twin A. CB4 nucleic acids were also amplified from blocks containing the adrenal glands and pancreases of both twins, although less amplification product was obtained compared to the brain or heart samples (Fig. S1). FFPE blocks that were PCR-positive but ISH-negative were interpreted as possibly the result of viremia.[6]

Using ISH and immunohistochemistry, we were able to detect viral RNA and protein in the heart, brain, adrenal glands, pancreas and spleen white pulp in both twins (Fig. 1C,F,I,L). Hybridization in heart tissue gave the most robust signal with greater than 10% of myocardiocytes demonstrating infection. In the brain, cortical neurons (Fig. 1F) and residual subependymal matrix cells (Fig. 2A) showed prominent CB4 ISH along with surrounding T-cell infiltration (Figs 1E,2B). Additionally, we observed viral infection in pancreatic islets of Langerhans (Figs 1L,3A), as well as discrete foci noted in the adrenal medulla (Figs 1I,2C), and in lymphoid follicles of the white pulp of the spleen (Figs 2D,3D).

To define the lineage of CB4 infected cells, we utilized combinations of double immunofluorescence (IF) and IF/ISH (Figs 2,3). In the adrenal gland, only medullary cells were infected and some of these co-localized with TH staining (Fig. 2C). Infected cells in the pancreas were limited to endocrine elements that labeled with antibodies to synaptophysin (Fig. 3A-C). Given the cell density of the spleen, it was more difficult to identify what element in the white pulp contained viral nucleic acids. Double-labelling with ISH for virus and CD21 for follicular dendritic cells showed co-localization (Figs 2D,3F). However, we performed ISH with both positive and negative sense probes, and only the negative sense probe hybridized (Fig. 2D). Therefore, the viral signal observed in the spleen is most likely entrapped virus and not infected cells.

Based on cell morphology and ISH, CB4 infected only a subset of neuronal elements. We observed viral RNA in germinal matrix elements (Fig. 2), as well as in neurons stained with MAP2 based on morphology (Fig. 3G-I). While our anti-enterovirus antibody revealed some non-specific binding in brain tissue as seen by others,[27] we matched IF signal with what we observed via ISH in order to accurately locate infected cells. None of the infected brain cells co-localized with GFAP or Iba1 staining. Virus infection within different CNS regions (Table 2) is illustrated in Figure S2.

DISCUSSION

Enteroviruses infect the host via oral or respiratory routes. After replication in regional lymph nodes of the upper respiratory or gastrointestinal tracts,[5,6] the virus enters the bloodstream and disseminates to systemic organs. For obvious reasons the time course and spread of virus in humans is less well known than in animal models. However, these twins clearly document the state of infection after dissemination and support the general pathogenesis model. While we did not detect CB4 via ISH in the respiratory or

gastrointestinal epithelium, low levels of viral nucleic acids were detected by PCR in RNA extracted from lung and gut tissues. Our inability to detect infected cells by ISH could be the result of limited sampling, time of sampling or alternatively those viral nucleic acids detected by PCR could reflect viremia in the non-perfused human tissues.

Given the severity of myocarditis, the immediate cause of death in the twins was probably CB4 infection of the myocardium. However, had they survived the myocardial insult, death from encephalitis would have been expected. Should the host survive or escape myocarditis and encephalitis, our findings of infection of endocrine pancreas might account for the incidence of type 1 diabetes associated with CB4 infection.[15]

Like other enteroviruses, most clinically significant coxsackie B virus infections occur in young children. This is most likely the result of their immature and naïve immune systems. In general, humoral immunity is thought to prevent severe systemic infection by picornaviruses. In the case of these newborn twins, presumably maternal immunoglobulin was insufficient to provide protection either because the mother had a limited titer or because the children were not breastfed. With exposure to multiple enteroviruses, adaptive immune responses provide protection to both infecting and genetically related viruses. Thus adults tend to have less severe disease because of specific and heterosubtypic immunity. However, the severe infection in newborns may not be purely a function of immune competence but may also reflect relative abundance of a developmentally regulated viral receptor.

The coxsackievirus and adenovirus receptor (CAR) is a well-established type 1 membrane receptor for group B coxsackieviruses and subgroup C adenoviruses. CAR distribution varies across tissues but is highly expressed in prostate,thyroid,testis,pituitary gland and the developing brain. Previous studies have demonstrated that enteroviruses infect the endocrine but not the exocrine pancreas, specifically beta cells of the islets, which express CAR.[18] We detected infection in only a subset of these tissues, namely the brain and pancreas (Tables 1,2). This may in part be due to the fact that CAR expression is developmentally regulated and distribution in infant and adult humans is not explicitly known. In the nervous system, CAR is strongly expressed during embryogenesis and is drastically reduced at early postnatal stages.[28] Additionally, CAR expression has been shown in neural crest elements in both animal models and human embryonic stem cells,[29,30] which matches our observations of adrenal medulla and pancreatic islet cell infection. Therefore, the distribution of CB4 infected cells we observed in these twins may be the result of differential CAR expression.

Animal studies have suggested that the preferential expression of cellular receptors on newborn mouse brain cells might be related to their high susceptibility to CB3 infection, as compared to adult mice with dramatically reduced receptor expression.[31] Tissue-specific CAR gene deletion in 6–8-week-old mice significantly reduces virus titers, as well as virus-induced tissue damage and inflammation in the heart and pancreas when infected with CB3.[32,33] Using recombinant CB3 tagged with enhanced green fluorescent protein,[34] others have shown an age-dependent loss of susceptibility to infection in neonatal mice. While newborn mice were readily infected, by 1 week of age, mice exhibited no mortality after intracranial infection and by 1 month no infectious virus could be recovered (although viral

RNA was detectable).[35] Infected cells labeled with nestin, were distributed in a pattern consistent with stem elements. Additional labeling and bone marrow transplantation experiments suggested that some of these stem-related elements were recruited to the CNS by local expression of chemokine (C-C motif) ligand 12 (CCL12).[36] These findings are reminiscent of our observation of infected residual germinal matrix in the brains of the twins, suggesting expression of CAR or some other factor may make these stem elements susceptible to CB4 infection.

The distribution and kinetics of CB4 infection in the two twins is difficult to discern from the autopsies alone. However, the relative abundance of inflammation and viral infected cells suggests an interesting dynamic. If both infants were infected around the same time, then infant A, who died 2 days earlier, might represent an earlier stage of infection than infant B. The severity of histopathology is consistent with this hypothesis. In both infants, inflammatory lesions in the CNS were more widely distributed than viral nucleic acids (Table 2). Particularly in the spinal cord and brainstem, the degree of inflammatory infiltrate far outstretched the abundance of CB4 nucleic acids as seen with other enteroviruses.[37-41] This would suggest that the temporal pattern of CB4 spread in the nervous system began in the cord and ascended to more rostral levels. Additionally we hypothesize that the inflamed spinal cord regions are consistent with an early viral clearance by the time of death. Perusing Table 2 suggests that viral infection of the caudal CNS had begun to abate by the time of death. The inflammatory response in the spinal cord and brainstem in the absence of much detectable CB4 nucleic acids suggests that either the nascent immune response or maturation of innate immunity resulted in regional “clearance” of the virus. Whether viral clearance is the result of destruction of target host cells or a decrease in their susceptibility to productive infection would be a matter of conjecture. However, recent studies in other viral systems[42,43] suggest that neuronal-specific regulation of toll-like receptors[44] can account for differential susceptibility to viral infection.

Currently there is no vaccination or effective therapy for coxsackievirus infection. While symptoms are generally mild, resulting in a flu-like illness, neonates in particular are susceptible to a severe disease progression. The two twins reported here died of myocarditis and encephalitis; however, infection of other organs (e.g. endocrine pancreas) could account for significant morbidity during less severe infections. Greater understanding of the pathogenesis of CB4 infection would be instrumental in devising protective strategies.

Supplementary Material

Refer to Web version on PubMed Central for supplementary material.

Acknowledgments

We would like to thank Mark Stauffer and Arlene Carbone-Wiley for their valuable technical assistance. These studies received partial support from NIH NIAID grant U01 AI 111598.

REFERENCES

1. Tyler, KL.; Martin, JB. Infectious Diseases of the Central Nervous System. F.A. Davis; Philadelphia, PA: 1993.

2. Berger JR, Chumley W, Pittman T, Given C, Nuovo G. Persistent Coxsackie B encephalitis: report of a case and review of the literature. J Neurovirol. 2006; 12:511–516. [PubMed: 17162666]

3. Bryant PA, Tingay D, Dargaville PA, Starr M, Curtis N. Neonatal coxsackie B virus infection-a treatable disease? Eur J Pediatr. 2004; 163:223–228. [PubMed: 14986123]

4. Callen J, Paes BA. A case report of a premature infant with coxsackie B1 meningitis. Adv Neonatal Care. 2007; 7:238–247. [PubMed: 18049150]

5. Solomon T, Lewthwaite P, Perera D, Cardoso MJ, McMinn P, Ooi MH. Virology, epidemiology, pathogenesis, and control of enterovirus 71. Lancet Infect Dis. 2010; 10:778–790. [PubMed: 20961813]

6. Zaoutis T, Klein JD. Enterovirus infections. Pediatr Rev. 1998; 19:183–191. [PubMed: 9613170]

7. Centres for Disease Control (CDC). Nonpolio enterovirus and human parechovirus surveillance – United States, 2006–2008. MMWR Morb Mortal Wkly Rep. 2010; 59:1577–1580. [PubMed: 21150865]

8. Moore M, Kaplan MH, McPhee J, Bregman DJ, Klein SW. Epidemiologic, clinical, and laboratory features of Coxsackie B1-B5 infections in the United States, 1970–79. Public Health Rep. 1984; 99:515–522. [PubMed: 6091168]

9. Brecht M, Jyoti R, McGuire W, Chauhan M. A case of neonatal coxsackie B virus brainstem encephalitis. J Paediatr Child Health. 2010; 46:699–701. [PubMed: 21077981]

10. Berger JR, Fee DB, Nelson P, Nuovo G. Coxsackie B meningoencephalitis in a patient with acquired immunodeficiency syndrome and a multiple sclerosis-like illness. J Neurovirol. 2009; 15:282–287. [PubMed: 19444695]

11. David P, Baleriaux D, Bank WO, et al. MRI of acute disseminated encephalomyelitis after coxsackie B infection. J Neuroradiol. 1993; 20:258–265. [PubMed: 8308544]

12. Kamei S, Hersch SM, Kurata T, Takei Y. Coxsackie B antigen in the central nervous system of a patient with fatal acute encephalitis: immunohistochemical studies of formalin-fixed paraffin-embedded tissue. Acta Neuropathol (Berl). 1990; 80:216–221. [PubMed: 2167606]

13. Estes ML, Rorke LB. Liquefactive necrosis in Coxsackie B encephalitis. Arch Pathol Lab Med. 1986; 110:1090–1092. [PubMed: 3022671]

14. Iwasaki T, Monma N, Satodate R, Kawana R, Kurata T. An immunofluorescent study of generalized Coxsackie virus B3 infection in a newborn infant. Acta Pathol Jpn. 1985; 35:741–748. [PubMed: 2994361]

15. Berg AK, Olsson A, Korsgren O, Frisk G. Antiviral treatment of Coxsackie B virus infection in human pancreatic islets. Antiviral Res. 2007; 74:65–71. [PubMed: 17239967]

16. Dotta F, Censini S, van Halteren AG, et al. Coxsackie B4 virus infection of beta cells and natural killer cell insulitis in recent-onset type 1 diabetic patients. Proc Natl Acad Sci U S A. 2007; 104:5115–5120. [PubMed: 17360338]

17. Foulis AK, Liddle CN, Farquharson MA, Richmond JA, Weir RS. The histopathology of the pancreas in type 1 (insulin-dependent) diabetes mellitus: a 25-year review of deaths in patients under 20 years of age in the United Kingdom. Diabetologia. 1986; 29:267–274. [PubMed: 3522324]

18. Ylipaasto P, Klingel K, Lindberg AM, et al. Enterovirus infection in human pancreatic islet cells, islet tropism in vivo and receptor involvement in cultured islet beta cells. Diabetologia. 2004; 47:225–239. [PubMed: 14727023]

19. Burch GE, DePasquale NP, Sun SC, Mogabgab WJ, Hale AR. Endocarditis in mice infected with Coxsackie virus B4. Science. 1966; 151:447–448. [PubMed: 5902385]

20. Hoshino T, Kawai C, Tokuda M. Experimental coxsackie B viral myocarditis in cynomolgus monkeys. Jpn Circ J. 1983; 47:59–66. [PubMed: 6298479]

21. Lansdown AB. Pathological changes in the pancreas of mice following infection with Coxsackie B viruses. Br J Exp Pathol. 1976; 57:331–338. [PubMed: 782500]

22. Al-Hello H, Davydova B, Smura T, et al. Phenotypic and genetic changes in coxsackievirus B5 following repeated passage in mouse pancreas in vivo. J Med Virol. 2005; 75:566–574. [PubMed: 15714484]

23. Palacios G, Oberste MS. Enteroviruses as agents of emerging infectious diseases. J Neurovirol. 2005; 11:424–433. [PubMed: 16287683]

24. Bissel SJ, Wang G, Ghosh M, et al. Macrophages relate presynaptic and postsynaptic damage in simian immunodeficiency virus encephalitis. Am J Pathol. 2002; 160:927–941. [PubMed: 11891191]
25. Fallert BA, Reinhart TA. Improved detection of simian immunodeficiency virus RNA by in situ hybridization in fixed tissue sections: combined effects of temperatures for tissue fixation and probe hybridization. J Virol Methods. 2002; 99:23–32. [PubMed: 11684300]
26. Bissel SJ, Giles BM, Wang G, Olevian DC, Ross TM, Wiley CA. Acute murine H5N1 influenza A encephalitis. Brain Pathol. 2012; 22:150–158. [PubMed: 21714828]
27. Jia CS, Liu JN, Li WB, et al. The cross-reactivity of the enterovirus 71 to human brain tissue and identification of the cross-reactivity related fragments. Virol J. 2010; 7:47. [PubMed: 20170551]
28. Patzke C, Max KE, Behlke J, et al. The coxsackievirus-adenovirus receptor reveals complex homophilic and heterophilic interactions on neural cells. J Neurosci. 2010; 30:2897–2910. [PubMed: 20181587]
29. Hotta Y, Honda T, Naito M, Kuwano R. Developmental distribution of coxsackie virus and adenovirus receptor localized in the nervous system. Brain Res Dev Brain Res. 2003; 143:1–13.
30. Brokhman I, Pomp O, Fishman L, et al. Genetic modification of human embryonic stem cells with adenoviral vectors: differences of infectability between lines and correlation of infectability with expression of the coxsackie and adenovirus receptor. Stem Cells Dev. 2009; 18:447–456. [PubMed: 18554086]
31. Xu R, Crowell RL. Expression and distribution of the receptors for coxsackievirus B3 during fetal development of the Balb/c mouse and of their brain cells in culture. Virus Res. 1996; 46:157–170. [PubMed: 9029788]
32. Kallewaard NL, Zhang L, Chen JW, Guttenberg M, Sanchez MD, Bergelson JM. Tissue-specific deletion of the coxsackievirus and adenovirus receptor protects mice from virus-induced pancreatitis and myocarditis. Cell Host Microbe. 2009; 6:91–98. [PubMed: 19616768]
33. Shi Y, Chen C, Lisewski U, et al. Cardiac deletion of the Coxsackievirus-adenovirus receptor abolishes Coxsackievirus B3 infection and prevents myocarditis in vivo. J Am Coll Cardiol. 2009; 53:1219–1226. [PubMed: 19341864]
34. Feuer R, Mena I, Pagarigan R, Slifka MK, Whitton JL. Cell cycle status affects coxsackievirus replication, persistence, and reactivation in vitro. J Virol. 2002; 76:4430–4440. [PubMed: 11932410]
35. Feuer R, Mena I, Pagarigan RR, Harkins S, Hassett DE, Whitton JL. Coxsackievirus B3 and the neonatal CNS: the roles of stem cells, developing neurons, and apoptosis in infection, viral dissemination, and disease. Am J Pathol. 2003; 163:1379–1393. [PubMed: 14507646]
36. Tabor-Godwin JM, Ruller CM, Bagalso N, et al. A novel population of myeloid cells responding to coxsackievirus infection assists in the dissemination of virus within the neonatal CNS. J Neurosci. 2010; 30:8676–8691. [PubMed: 20573913]
37. Chan LG, Parashar UD, Lye MS, et al. For the Outbreak Study Group. Deaths of children during an outbreak of hand, foot, and mouth disease in sarawak, malaysia: clinical and pathological characteristics of the disease. Clin Infect Dis. 2000; 31:678–683. [PubMed: 11017815]
38. Wong KT, Munisamy B, Ong KC, et al. The distribution of inflammation and virus in human enterovirus 71 encephalomyelitis suggests possible viral spread by neural pathways. J Neuropathol Exp Neurol. 2008; 67:162–169. [PubMed: 18219253]
39. Yan JJ, Wang JR, Liu CC, Yang HB, Su IJ. An outbreak of enterovirus 71 infection in Taiwan 1998: a comprehensive pathological, virological, and molecular study on a case of fulminant encephalitis. J Clin Virol. 2000; 17:13–22. [PubMed: 10814934]
40. Yang Y, Wang H, Gong EC, et al. Neuropathology in 2 cases of fatal enterovirus type 71 infection from a recent epidemic in the People's Republic of China: a histopathologic, immunohistochemical, and reverse transcription polymerase chain reaction study. Hum Pathol. 2009; 40:1288–1295. [PubMed: 19386354]
41. Zhang YC, Jiang SW, Gu WZ, et al. Clinicopathologic features and molecular analysis of enterovirus 71 infection: report of an autopsy case from the epidemic of hand, foot and mouth disease in China. Pathol Int. 2012; 62:565–570. [PubMed: 22827767]

42. Lafaille FG, Pessach IM, Zhang SY, et al. Impaired intrinsic immunity to HSV-1 in human iPSC-derived TLR3-deficient CNS cells. Nature. 2012; 491:769–773. [PubMed: 23103873]

43. Zhang SY, Jouanguy E, Ugolini S, et al. TLR3 deficiency in patients with herpes simplex encephalitis. Science. 2007; 317:1522–1527. [PubMed: 17872438]

44. Ma Y, Haynes RL, Sidman RL, Vartanian T. TLR8: an innate immune receptor in brain, neurons and axons. Cell Cycle. 2007; 6:2859–2868. [PubMed: 18000403]

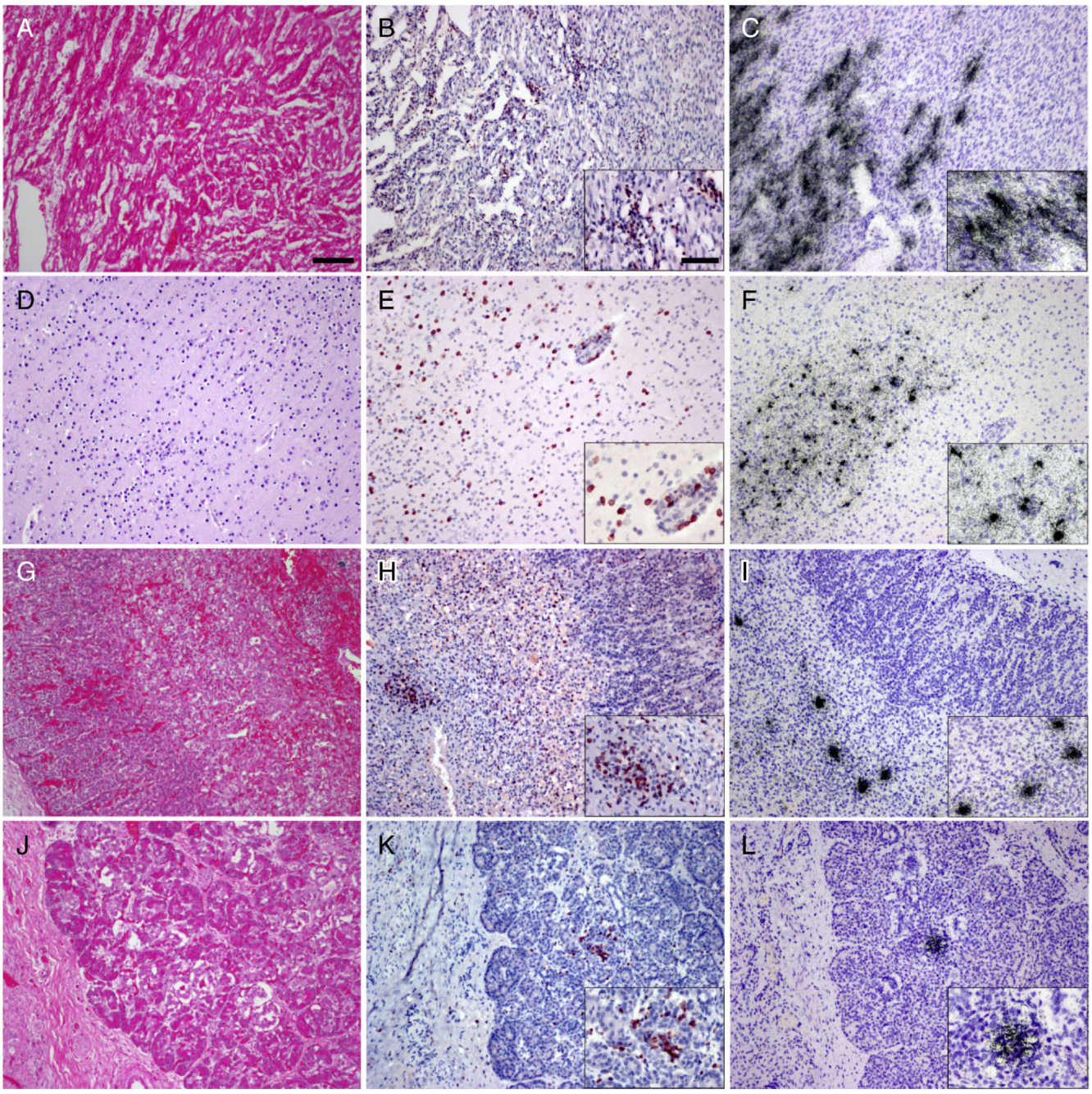

Fig. 1.

Histopathological analysis of autopsy tissues demonstrates widespread inflammation and infection. HE stains of the myocardium demonstrate severe edema and lymphocytic infiltration (A). Most infiltrating lymphocytes stain with an antibody to CD3 (B). *In situ* hybridization (ISH) for coxsackie B virus (CB4) (C) shows infection of cardiac myocytes in regions of inflammation. HE stains also demonstrate multifocal diffuse inflammation of brain parenchyma (D). Inflammatory cells in the brain predominantly stain with CD3 (E). ISH for CB4 (F) shows multifocal infection throughout the CNS. HE stain of the adrenal

gland (G) (M = medulla, C = cortex) shows mild inflammatory infiltrate of the medulla more readily appreciated after immunostaining for CD3 (H). ISH for CB4 (I) shows infection limited to adrenal medulla. Inflammation is difficult to appreciate on HE stained sections of pancreas (J) but T cell infiltration is clear after immunostaining for CD3 (K). ISH for CB4 (L) shows infection of discrete islands of cells in regions of inflammation. All images at 10× magnification with insets at 20×, bar in 10× = 100 μm, in 20× = 50 μm.

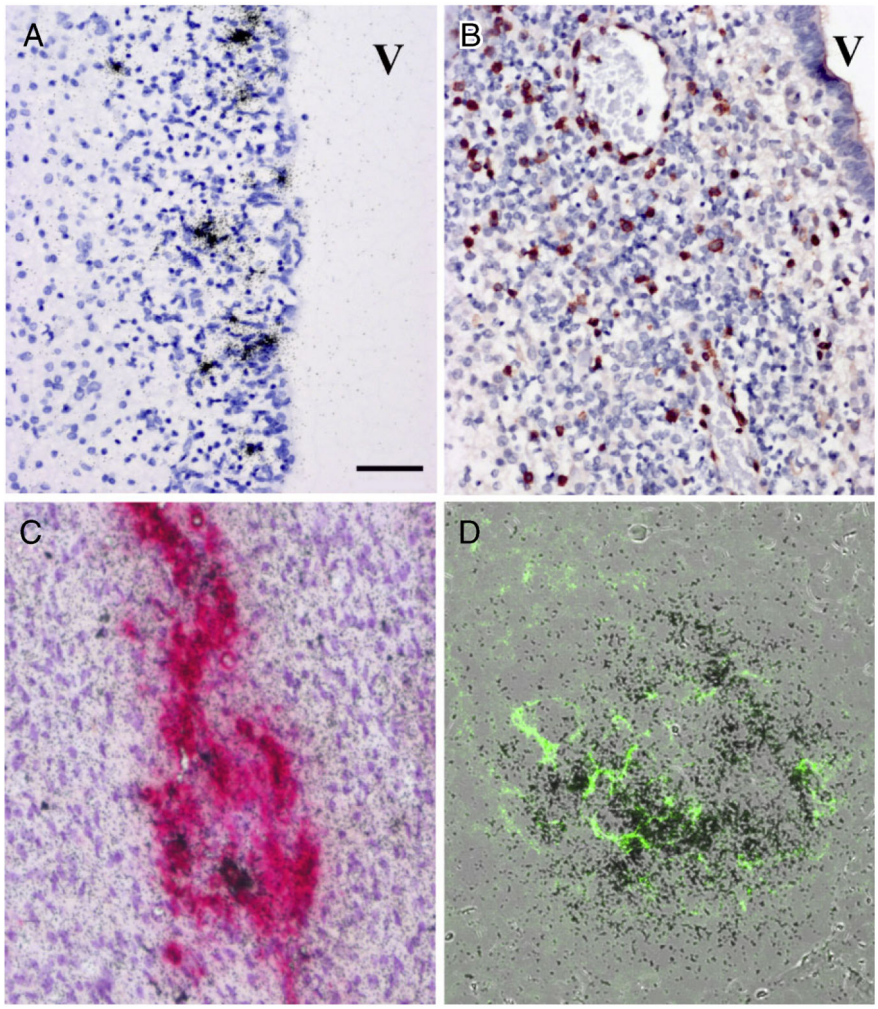

Fig. 2.

Histopathological assessment of brain, adrenal gland and spleen. Histopathological analysis of brain tissues demonstrates widespread inflammation and infection in germinal matrix (A,B). *In situ* hybridization (ISH) for coxsackie B virus (CB4) (A) shows infection of stem cell elements underlying ependymal lined ventricle (V). Immunocytochemistry for CD3 demonstrates diffuse infiltration of germinal matrix by T cells (B). Double-label immunocytochemistry and ISH for tyrosine hydroxylase (red) and CB4 RNA (black grains) of the adrenal medulla shows tyrosine hydroxylase positive cells, some of which co-label for viral RNA (C). Overlain images of ISH for viral RNA in spleen demonstrating abundant signal (black grains) in lymphoid follicles while a serial paraffin section defines CD21 staining (green) of follicular dendritic cells (D). All images at 20× magnification, bar = 50 μm.

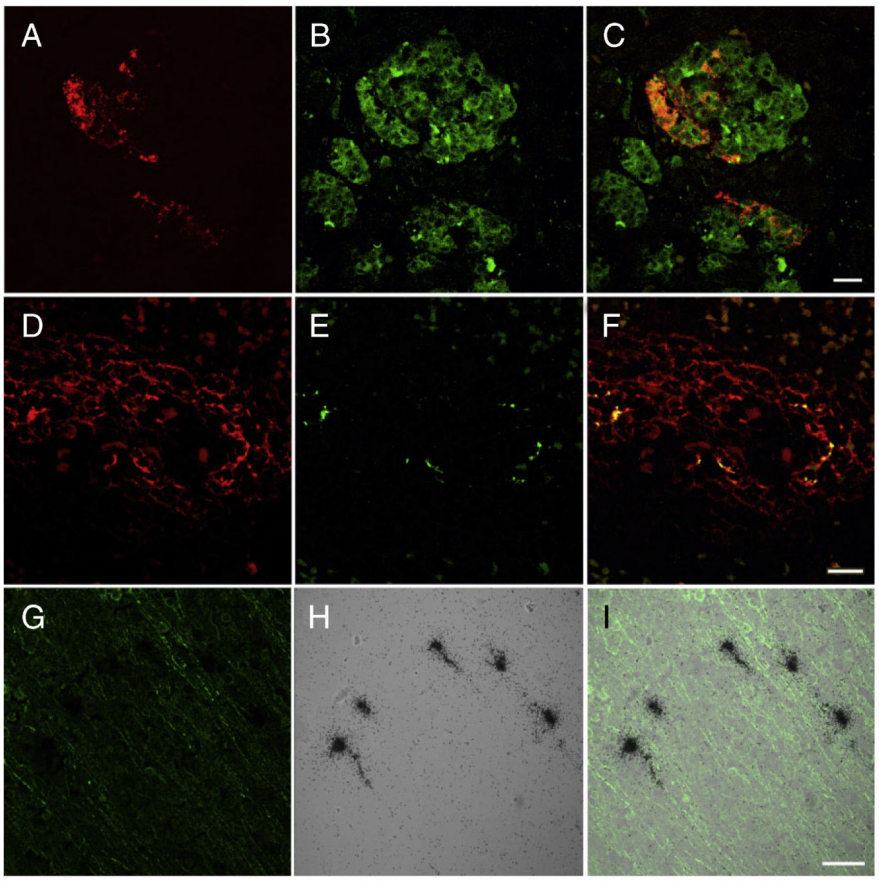

Fig. 3.

Double label immunocytochemistry for enterovirus (red) (A) and synaptophysin (green) (B) demonstrate infection of individual cells in the islets of Langerhans shown in the merged image (C). Double-label immunocytochemistry of spleen for CD21 (red) (D) and enterovirus (green) (E) demonstrated co-localization within follicles shown in the merged image (F). *In situ* hybridization with sense and anti-sense probes demonstrates that spleen signal was limited to detecting entrapped virion without detecting infected cells (see results). Double-label immunocytochemistry for microtubule-associated protein 2 (MAP2) (green) (G) and *in situ* hybridization for coxsackie B virus (CB4) (black grains) (H) demonstrates infection of cortical neurons shown in the merged image (I).A–F bar = 20 μm, G–I bar = 50 μm.

Table 1

Tissue distribution of CB4 infected cells

Tissue	Tissue distribution of CB4 infection				
	Twin A		Twin B		cell type
	PCR	ISH	PCR	ISH	
Heart	+	+	+	+	Myocardiocytes
Lung	+/−	−	−	−	NA
Trachea	+	−	+/−	−	NA
Esophagus	−	−	+/−	−	NA
Stomach	−	−	na	na	NA
Small intestine	+/−	−	−	−	NA
Large intestine	na	na	−	−	NA
Genitourinary	−	−	na	na	NA
Liver	+/−	−	−	−	NA
Spleen	+	+	−	+	Follicular dendritic cell
Pancreas	+	+	+	+	Islets of Langerhans
Kidney	+	−	−	−	NA
Adrenal	+	+	+	+	Adrenal medulla
Thymus	−	−	na	na	NA
Thyroid	na	−	+/−	−	NA
Prostate	na	−	+	−	NA
Testis	na	−	na	na	NA

PCR and in situ hybridization (ISH) were performed on formalin-fixed paraffin-embedded tissues from the autopsies of both twins. Strong ethidium bromide bands of PCR amplified products were identified in many tissues (+) while weak (+/−) or no (−) bands were detected in other tissues (Fig. S1). ^{35}S viral ISH positive infected cells were identified in a more limited number of tissues. Weak PCR signal in tissues that were ISH negative may represent viremia. CB4, coxsackie B virus; NA, not applicable; na, not available.

Table 2

CNS distribution of CB4 infection and CD3 infiltration

Tissue	CNS distribution of CB4 infection and CD3 infiltration							
	Twin A				Twin B			
	CD3 infiltration	PCR	ISH	Cell infected	CD3 infiltration	PCR	ISH	Cell infected
Mid frontal cortex	++	+	+	CN	+++	+	+	CN
Caudate and cingulate	++	+	+	SGM	++	+	+	CN, SGM
Striatum	++	+	+	SGM	+++	+	+	DGMN, SGM
Thalamus	+	+	−	NA	+++	+	+	DGMN, SGM
Hippocampus	+	−	+	CN, CP, SGM	+++	−	+	CN
Cerebellum	+++	−	+	CP, DGMN	+	−	−	NA
Midbrain	+++	+	+	SGM, DGMN	+++	−	−	NA
Pons	+	−	−	NA	++	−	−	NA
Medulla	+	−	−	NA	+++	na	−	NA
Spinal cord	++	−	−	NA	na	na	na	na
Pituitary	na	na	na	na	++	+	+	Anterior pituicytes

Severity of CD3 cell infiltration in different regions of the CNS was assessed on the basis of immunocytochemistry on a scale of 0 to +++ (none, mild, moderate and severe). PCR for CB4 was performed on cDNA derived from RNA extracted from FFPE tissue sections. Blocks showing amplified PCR bands in ethidium bromide stained agarose gel were rated + while those not showing bands were rated −. *In situ* hybridization for CB4 was performed on FFPE tissue sections. Blocks showing any cells that hybridized for CB4 were rated + while those not showing any infected cells were rated −. The identity of infected cells was determined on the basis of morphology. CB4, coxsackie B virus; FFPE, formalin-fixed paraffin-embedded; SGM, subependymal germinal matrix cells; CP, choroid plexus cells; DGMN, deep cortical gray matter neurons; CN, cortical neurons; NA, not applicable; na, not available.